

The shear and extensional rheology of xanthan gum and DUO-VIS

Janaki Umashanker¹, Bart Hallmark¹

¹University of Cambridge, Philippa Fawcett Drive, Cambridge CB3 0AS

ABSTRACT

The shear and extensional rheology of aqueous solutions of xanthan gum, concentration 5 g/L, and DUO-VIS, a xanthan based viscosifier, at a concentration of 5 g/L, have been explored experimentally. The rheological data had shown viscoelasticity, shear thinning, with DUO-VIS also showing possible presence of a yield stress.

The Carreau-Yasuda and Herschel-Bulkley models fitted well with the steady shear data. The viscoelastic response of xanthan gum was captured in shear and extension using a two mode Giesekus model, using the same Giesekus parameters. This was inhibited for DUO-VIS by the presence of “beads on a string” during capillary break-up experiments.

INTRODUCTION

Drilling is a common operation that has historically been used to facilitate the extraction of oil and gas resources. Looking to the future, drilling has an important role to play in carbon capture and storage, since bores will need to be drilled into geologically suitable formations for carbon dioxide sequestration.

During the construction of a wellbore, a drill bit is used to drill into the rock beneath. A fluid, known as a drilling fluid, is circulated around the well to remove these cuttings to the surface, maintain formation pressure for stability and a selection of other functions. At the end of each section drilled, a large diameter steel pipe, known as casing,

is cemented into the wellbore. To keep the drilling fluids and cement apart, spacer fluids are used during the displacement to prevent contamination.

These fluids, known as well construction fluids (WCFs), are subjected to a variety of processing conditions during operations. The material response of these WCFs in both shear and extension is an essential component of their overall efficacy during the drilling process. A thorough understanding of the rheological behaviour of WCFs in both shear and extension is, therefore, required.

This paper explores the shear and extensional rheology of a biopolymer solution commonly encountered in WCFs, xanthan gum. Also explored is DUO-VIS¹, a xanthan gum viscosifier, which is used as an additive in aqueous drilling and spacer fluids.

MATERIALS AND METHODS

Xanthan gum (Sigma Aldrich) is a hydrocolloid and is soluble in water. The concentration studied was 5 g/L, which is within the semi dilute regime. Aqueous solutions of xanthan gum in deionised water were prepared following the procedure highlighted by Martin-Alfonso and co-workers².

DUO-VIS powder (M-I SWACO) was made up for an aqueous solution at 5 g/L concentration. Preparation followed the same procedure as xanthan gum² but had a mixing time of 24 hours.

All rheometry tests were carried out at 20° C.

RHEOMETERS

Shear rheometers

Two rotational rheometers were used to obtain steady shear and oscillatory data: the ARES (Rheometric Scientific Inc.) and the Kinexus (Malvern Instruments Ltd.). Xanthan gum was tested on the ARES rheometer using a cone and plate geometry, with DUO-VIS being tested on the Kinexus using roughened parallel plates. Roughened plates were used with DUO-VIS since previous experiments had shown that it was prone to slip.

The cone and plate used on the ARES had a plate diameter of 50 mm, plate truncation gap of 0.051 mm and cone angle of 0.04 radians. The diameter of the roughened parallel plates was 40 mm and was used with a gap of 1 mm.

To obtain rheological data at high shear rates, a capillary rheometer was used. The Cambridge Multipass Rheometer (MPR, Strata Technology Ltd.) was used to investigate shear rates ranging between 500 s^{-1} and $100,000 \text{ s}^{-1}$. The geometries used for both xanthan gum and DUO-VIS were cylindrical capillaries of diameter 1 mm, and lengths 4 mm, 10 mm and 20 mm. Experiments using several different capillary dimensions were required to obtain data for the capillary rheometer correction factors³.

Extensional rheometer

The Trimaster HB4 (Huxley Bertram Ltd.) was used to investigate the extensional rheology of both solutions. The HB4 is a capillary break-up device, which measures the diameter of a stretched fluid filament as it thins under the action of surface tension.

In use, a sample of fluid was placed in a 0.6 mm gap between two pistons, 1.2 mm in diameter. The pistons were then pulled apart at a velocity of 1 m/s until their separation distance was 1.6 mm. The filament of fluid that formed was filmed using a high-speed camera (Photron Fastcam 1024 PCI), operating at 18,000 frames per second with

shutter speed $1.1 \times 10^{-5} \text{ s}$. The camera resolution was 14.6 pixels per μm . Quantitative data for the change of filament diameter as a function of time was calculated as a post processing step by using the Trivision image analysis software.

RHEOLOGICAL MODELS

Generalised Newtonian model

The Carreau-Yasuda (CY) model was used to describe the shear thinning nature of xanthan gum and DUO-VIS. This model is a generalised Newtonian model that assumes an absence of yielding behaviour and does not consider any time-dependent material response, such as elasticity. It is best suited for fluids having a plateau viscosity at both low and high shear rates. The CY model is given in Eq. 1.

$$\eta_{CY}(\dot{\gamma}) = \eta_{\infty} + (\eta_0 - \eta_{\infty})[1 + (\dot{\gamma}\lambda)^a]^{-\frac{n-1}{a}} \quad (1)$$

Here:

η_{CY} = Apparent shear viscosity (Pa.s)

$\dot{\gamma}$ = Shear rate (s^{-1})

η_{∞} = High shear rate viscosity (Pa.s)

η_0 = Low shear rate viscosity (Pa.s)

λ = Relaxation time (s)

a and n = Exponential factors

Viscoplastic model

The Herschel-Bulkley (HB) model assumes that a yield stress is required for flow to commence, after which the fluid behaves in a power-law manner. In common with the CY model, the HB model does not describe any time-dependent material behaviour. The HB model is shown in Eq. 2.

$$\sigma_{HB} = \sigma_0 + K\dot{\gamma}^n \quad (2)$$

Here:

σ_{HB} = Herschel-Bulkley shear stress (Pa)

σ_0 = Yield stress (Pa)

K = Consistency index ($\text{Pa}\cdot\text{s}^n$)

n = Power law index

Viscoelastic model

Many different viscoelastic models exist, which can be used to describe both linear and non-linear behaviour in steady shear. The shear thinning nature of both fluids in this paper requires use of non-linear viscoelastic model, of which the Giesekus model⁴ is one of the simplest in differential form. The Giesekus model is used to describe packed polymer chains dispersed in a Newtonian solvent. A general statement of the Giesekus model, neglecting the stress contribution from the solvent, is shown in Eq. 3.

$$\frac{\boldsymbol{\tau}}{\lambda} + \frac{\partial \boldsymbol{\tau}}{\partial t} + \mathbf{v} \nabla \boldsymbol{\tau} - ((\nabla \mathbf{v})^T \boldsymbol{\tau} + \boldsymbol{\tau} (\nabla \mathbf{v})) = -\frac{\eta_0}{\lambda} \dot{\boldsymbol{\gamma}} + \frac{a_G}{\eta_0} \boldsymbol{\tau} \cdot \boldsymbol{\tau} \quad (3)$$

Here:

- η_0 = Zero shear rate viscosity (Pa.s)
- a_G = Mobility factor
- λ = Relaxation time (s)
- $\boldsymbol{\tau}$ = Stress tensor (Pa)
- \mathbf{v} = Velocity vector (m/s)
- t = Time (s)
- $\dot{\boldsymbol{\gamma}}$ = $\nabla \mathbf{v} + \nabla \mathbf{v}^T$ – shear rate tensor (s⁻¹)

Solutions to Eq. 3 are presented in the literature for different flow fields. Two flow fields relevant to this study are steady shear, and uniaxial extension.

In steady shear, $\dot{\boldsymbol{\gamma}} = \dot{\gamma}_{xy} \begin{bmatrix} 0 & 1 & 0 \\ 1 & 0 & 0 \\ 0 & 0 & 0 \end{bmatrix}$. It can be shown that the steady shear viscosity predicted by Eq. 3, η_G , can be written as Eq. 4⁵.

$$\eta_G = \eta_0 \frac{(1-f_G)^2}{1+(1-2a_G)f_G} \quad (4)$$

Here:

$$f_G = \frac{1-X_G}{1+(1-2a_G)X_G} \quad (5)$$

$$X_G^2 = \frac{-1 + \sqrt{1 + 16a_G(1-a_G)(\lambda\dot{\gamma})^2}}{8a_G(1-a_G)(\lambda\dot{\gamma})^2} \quad (6)$$

The behaviour of some fluids, especially those with a range of molecular weights,

cannot be captured accurately with a single relaxation time. Multiple relaxation times can be used with the Giesekus model by rewriting Eq. 3 in multimode form, with $\boldsymbol{\tau} = \sum_i \boldsymbol{\tau}_i$. It is assumed that the i^{th} relaxation mode has different values of $\eta_{0,i}$, λ_i and a_i . It can be shown that the steady shear viscosity is given by a sum of terms as follows:

$$\eta_G = \sum_i \frac{\eta_{0,i}(1-f_{G,i})^2}{1+(1-2a_{G,i})f_{G,i}} \quad (7)$$

Here, $f_{G,i}$ simply refers to Eq. 5 calculated with parameters specific to the i^{th} relaxation mode which, in turn, relies on Eq. 6 used in a similar manner.

$$\text{In uniaxial extension, } \dot{\boldsymbol{\gamma}} = \dot{\gamma}_{zz} \begin{bmatrix} -\frac{1}{2} & 0 & 0 \\ 0 & -\frac{1}{2} & 0 \\ 0 & 0 & 1 \end{bmatrix}.$$

A solution to Eq. 3 can be derived that predicts the normalised diameter of a fluid filament, D/D_0 , thinning as a function of time, t , under the action of surface tension alone. The result is given in Eq. 8⁶.

$$\frac{t}{\lambda} = (4a_G - 3) \ln \left(\frac{\left(\frac{D}{D_0}\right) + \frac{2a_G\lambda\alpha}{D_0\eta_0}}{1 + \frac{2a_G\lambda\alpha}{D_0\eta_0}} \right) - \frac{2\eta_0 D_0}{\alpha\lambda} \left(\frac{D}{D_0} - 1 \right) \quad (8)$$

Here:

- D_0 = Initial filament diameter (m)
- α = Surface tension (N/m)

Extending the filament thinning analysis to multiple relaxation modes is non-trivial, and results in an ordinary differential equation (ODE) that requires numerical solution. Pistre and co-workers⁷ derived an ODE for dual mode filament thinning: their result is given in Eq. 9.

$$\frac{dD}{dt} = \frac{-\lambda_1\lambda_2(a_{G,1}\eta_{0,2}\boldsymbol{\tau}_{zz,1}^2 + a_{G,2}\eta_{0,1}\boldsymbol{\tau}_{zz,2}^2) - \eta_{0,1}\eta_{0,2}(\lambda_2\boldsymbol{\tau}_{zz,1} + \lambda_1\boldsymbol{\tau}_{zz,2})}{\eta_{0,1}\eta_{0,2}\lambda_1\lambda_2 \left(\frac{6\alpha}{D^2} + \frac{4}{D} \left(\frac{\lambda_2\eta_{0,1} + \lambda_1\eta_{0,2}}{\lambda_1\lambda_2} \right) \right)} \quad (9)$$

Here:

$$\tau_{zz} = \text{Axial extra stress tensor (Pa)}$$

RESULTS AND DISCUSSION

Shear rheometry and classification

Flow curves showing the apparent shear viscosity as a function of shear rate for both xanthan gum and DUO-VIS, obtained from rotational and capillary rheometry, are shown in Fig. 1. Also included in this plot is the CY model fitted to both data sets.

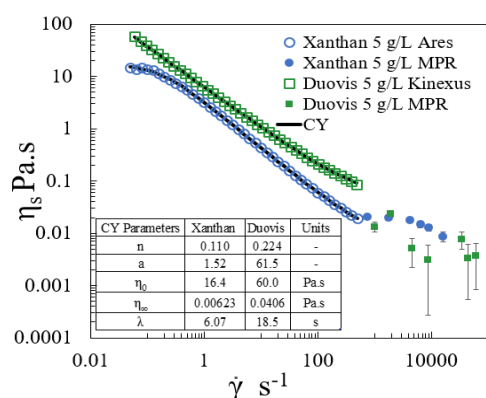


Figure 1: Apparent viscosity as a function of shear rate for xanthan gum (circles) and DUO-VIS (squares). Data obtained from rotational (open points) and capillary (closed points) rheometry.

MPR data for both fluids were corrected using the Rabinowitsch and Bagley corrections³. The maximum Reynolds number within the MPR was 0.01, indicating creeping, non-inertial, flow.

It can be seen from Fig. 1 that both fluids are prone to significant levels of shear thinning over the range of shear rates investigated. Shear thinning occurs in polymer solutions when the polymer chains start to disentangle, causing the viscosity of fluid to decrease with increasing shear rate.

Prior to shear thinning, xanthan gum displays a plateau viscosity at shear rates below about 0.3 s⁻¹. This behaviour matches existing literature data for the same concentration⁸. The coefficient of

determination, R^2 , between rotational rheometry data and the CY model for both xanthan gum and DUO-VIS is $R^2 = 0.99$.

The discontinuity between rotational and capillary data for xanthan gum is likely due to the presence of vortices at the entrance of the capillary. Li and co-workers⁹ demonstrate that vortices upstream of a contraction augment the pressure drop measured across the contraction. Apparent viscosity data yielded by capillary rheometry are derived from pressure drop measurements, hence the presence of vortices likely explain this viscosity mismatch.

The gradient of the flow curve for DUO-VIS is -0.75 over the range 0.01 < $\dot{\gamma}$ < 1000, possibly indicating the presence of a yield stress. Previous studies¹⁰ of DUO-VIS rheology have revealed the presence of a yield stress. Rheological data for DUO-VIS is replotted in Fig. 2 as stress as a function of shear rate. The data shown in Fig. 2 are not consistent with those of a yield stress fluid prior to yield, and more experimental data is required to investigate yielding.

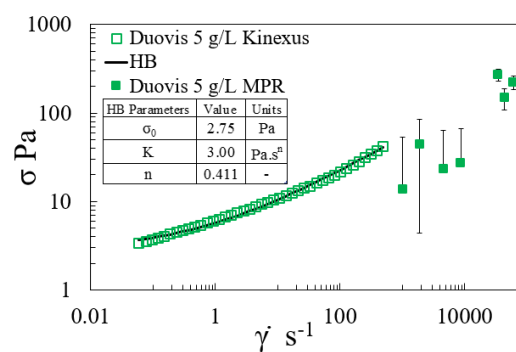


Figure 2: Shear stress as a function shear rate for DUO-VIS at 5 g/L. Data obtained from rotational (open points) and capillary (closed points) rheometry.

The coefficient of determination, R^2 , between rotational rheometry data and the HB model for DUO-VIS is $R^2 = 0.99$.

The discontinuity between rotational and capillary data for DUO-VIS shows the

opposite trend to that from xanthan gum. This could be explained by structural breakdown in the extensional flow field present in capillary rheometry, but more work is required to understand this behaviour.

Giesekus model for xanthan gum at 5 g/L in shear and extensional flow

The variation of elastic and viscous moduli as a function of frequency for xanthan gum and DUO-VIS is shown in Fig. 3.

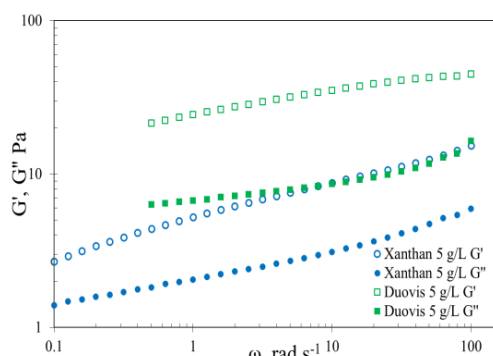


Figure 3: Variation of G' (open points) and G'' (closed points) as a function of angular frequency for xanthan gum (circles) and DUO-VIS (squares).

Fig. 3 clearly shows that $G' > G''$ over the range of angular frequencies tested, demonstrating that both xanthan gum and DUO-VIS are behaving predominantly elastically and that both fluids are viscoelastic. The xanthan gum behaviour is, again, consistent with that given in the literature^{2,6}. The presence of viscoelastic behaviour motivates the use of the Giesekus model to describe both the shear and extensional response of both fluids.

Fig. 4 and Fig. 5 present steady shear and filament thinning data for xanthan gum and compare these data to Eq. 4 and Eq. 8 respectively.

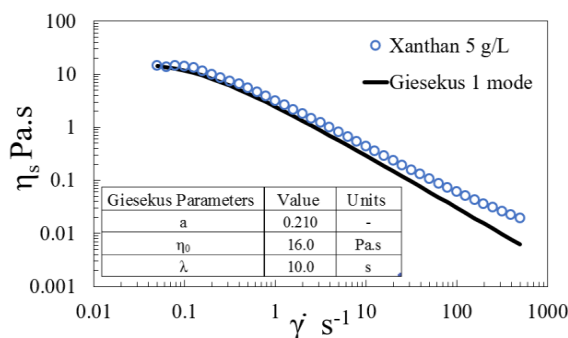


Figure 4: Apparent viscosity as a function of shear rate for xanthan gum obtained from rotational rheometry (data points) and locus of points from Eq. 4.

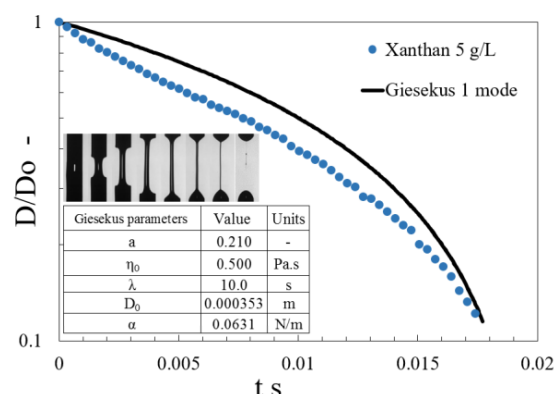


Figure 5: Normalised filament diameter as a function of time obtained from HB4 data (data points) and locus of points from Eq. 8.

The fit of Eq. 4 to the viscosity flow curve for xanthan gum shown in Fig. 4 is reasonably good, with $R^2 = 0.95$. There is divergence between the experimental data and Eq. 4 when $\dot{\gamma} > \sim 10 \text{ s}^{-1}$ indicating that a single relaxation mode cannot describe the full range of nonlinear behaviour in steady shear.

In Fig. 5, the images of the fluid filament during deformation show a cylindrical filament with a smooth surface that thins uniaxially over time. The rate of filament thinning is influenced by surface tension, inertia, elastic and viscous forces. For tests conducted on the HB4, the Reynolds number was 0.14, indicating that inertial forces are negligible.

Also shown in Fig. 5 is the locus of points due to Eq. 8 fitted with different parameters to those used for the shear data. This locus of points fails to capture the qualitative trend of the filament thinning data due to the presence of a point of inflection at about 6 ms. Previous work⁷ has shown that inflection points in filament thinning data can be described by multiple relaxation times.

The filament break-up time shown in Fig. 5 is shorter than that in the existing literature⁸ despite the same concentration of xanthan gum being used. Interestingly, Choi and co-workers⁸ prepared xanthan gum samples for their rheological testing by heating gum solutions to 70° C. This protocol is likely to affect the polymer structure, hence rheological response, of the gum. Rochefort and co-workers¹¹, cite that the structure of xanthan gum is temperature-sensitive. Exposure to elevated temperature causes conformational changes within the backbone, from a helical to a coiled structure, significantly altering intermolecular associations and hence the rheological response. This observation also suggests that although DUO-VIS is based on xanthan gum, its measurably different rheological response is most likely linked to exposure to elevated temperatures during the manufacturing process. This had been highlighted by Gulrez and co-workers¹² where industrial treatment had affected the xanthan gum molecular interactions.

It is clear from data shown in Fig. 4 and Fig. 5 that the Giesekus constitutive equation with a single relaxation time cannot describe both the shear and extensional response of xanthan gum. The presence of the point of inflection in the filament thinning data shown in Fig. 5 motivates the use of two relaxation modes.

Fig. 6 and Fig. 7 present the same apparent viscosity and filament thinning data that was shown in Fig. 4 and Fig. 5. Now, however, a dual mode Giesekus model is used with Eq. 7 and Eq. 9 being used to fit the shear and extensional data respectively.

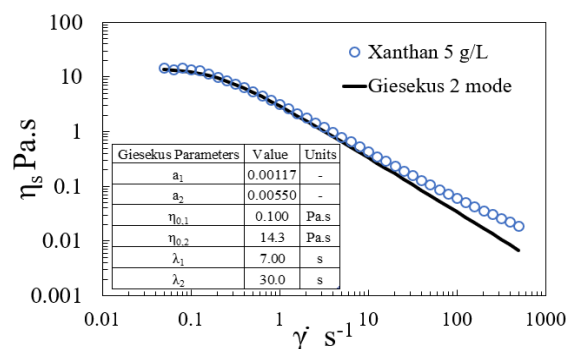


Figure 6: Apparent viscosity as a function of shear rate for xanthan gum obtained from rotational rheometry (data points) and locus of points from Eq. 7.

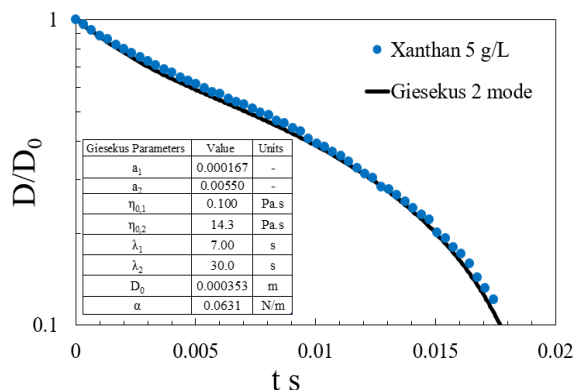


Figure 7: Normalised filament diameter as a function of time obtained from HB4 data (data points) and locus of points from Eq. 9.

The same set of Giesekus parameters is used in both shear and extension, demonstrating that two relaxation modes can provide a near-quantitative description of both shear and extensional behaviour of xanthan gum at 5 g/L. The coefficients of determination are $R^2 = 0.97$ and $R^2 = 0.99$ for Fig. 6 and Fig. 7 respectively. There is, however, still a slight divergence between Eq. 7 and the experimental data for $\dot{\gamma} > 10 \text{ s}^{-1}$, which may require more relaxation modes for a quantitative fit.

Extensional rheometry for DUO-VIS at 5 g/L

Filament thinning data for DUO-VIS is presented in Fig. 8.

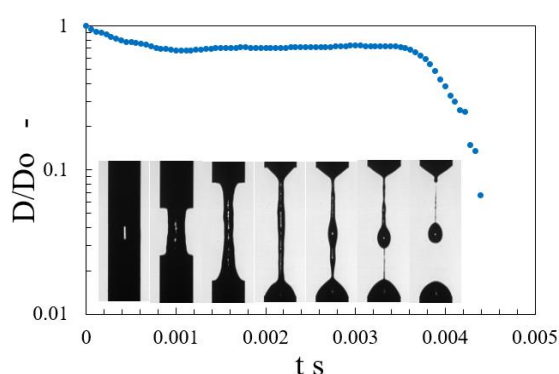


Figure 8: Normalised filament diameter of the narrowest part of the fluid filament as a function of time, along with representative images for DUO-VIS.

The filament thinning images in Fig. 8 initially show the presence of a rough, axisymmetric filament. After approximately 2 ms, an instability known as ‘beads-on-string’ (BOAS) occurs, with the filament breaking down into discrete droplets. This behaviour precludes the fitting of either Eq. 8 or Eq. 9 to the data, since both equations are derived under the assumption that the fluid filament always remains cylindrical.

Data shown in Fig. 1 indicated that DUO-VIS has high shear viscosity, possibly due to polymer aggregation and subsequent entanglement of polymer chains. The high levels of elasticity exhibited by the solution, as shown in Fig. 3, causes the polymer chains to recoil when being stretched. This, in turn, could lead to uneven thinning of the filament *i.e.* filament bridging. There are many examples of this phenomena for viscoelastic liquids in the literature^{13,14}, where unstable bridges are formed leading to the BOAS phenomenon.

In order to obtain useful extensional data for DUO-VIS, different sets of experiments are required. Future work will include the use of contraction flows having high levels of extensional strain, both for quantitative measurement and for flow visualisation.

CONCLUSIONS

Rheological data for xanthan gum at a concentration of 5 g/L has been successfully obtained in both shear and extension. Shear rheology for DUO-VIS at a concentration of 5 g/L has also been successfully obtained, but the presence of beads-on-a-string precluded the acquisition of quantitative extensional data.

The shear rheology of xanthan gum shows the presence of a low shear rate plateau followed by significant shear thinning. The Carreau-Yasuda model fitted the experimental data well with $R^2 = 0.99$. In shear experiments, DUO-VIS lacked a low shear rate viscosity plateau and proved to be strongly shear thinning with $d \ln \eta_s / d \ln \dot{\gamma} = -0.75$. This may be indicative of yield stress behaviour, but more experimental data is required. Consequently, the Herschel-Bulkley was fitted to quantify the shear behaviour of DUO-VIS with $R^2 = 0.99$.

Dynamic rheometry data indicated that both xanthan gum and DUO-VIS were highly viscoelastic with $G' > G''$ over the range $0.1 < \omega < 100$ rad/s. Motivated by this, the Gieskeus model using both one and two relaxation modes were fitted to the shear and extensional data of xanthan gum.

It was not possible to describe both shear and extensional behaviour of xanthan gum using a single relaxation mode, but both deformations were captured accurately using two relaxation modes. The same Giesekus parameters were used in both shear ($R^2 = 0.97$) and extension ($R^2 = 0.99$), giving confidence to use this model for further flow modelling.

ACKNOWLEDGMENTS

Funding for this project is gratefully acknowledged from EPSRC and Schlumberger Cambridge Research.

REFERENCES

- 1“DUO-VIS.” M-I SWACO, 2011.

²Martín-Alfonso J.e., Cuadri A.a., Berta M., and Stading M. “Relation between Concentration and Shear-Extensional Rheology Properties of Xanthan and Guar Gum Solutions.” *Carbohydrate Polymers* 181 (2018): 63–70.

³Mackley M. R., Marshall R. T. J., and Smeulders J. B. A. F. “The Multipass Rheometer.” *Journal of Rheology* 39, no. 6 (1995): 1293–1309.

⁴Giesekus H. “A Simple Constitutive Equation for Polymer Fluids Based on the Concept of Deformation-Dependent Tensorial Mobility.” *Journal of Non-Newtonian Fluid Mechanics*, 11 (1982): 69–109.

⁵Armstrong R. C., Hassager O., and Bird R.B. *Dynamics of Polymer Liquids*. New York: Wiley, 1977.

⁶Torres M. D., Hallmark B., Wilson D.I., and Hilliou L. “Natural Giesekus Fluids: Shear and Extensional Behavior of Food Gum Solutions in the Semidilute Regime.” *AIChE Journal* 60, no. 11 (2014): 3902–15.

⁷Hallmark B., D. Wilson D.I., and Pistre N. “Characterization of Extensional Rheological Filament Stretching with a Dual-Mode Giesekus Model.” *AIChE Journal* 62, no. 6 (2016): 2188–99.

⁸Choi H., Mitchell J.R., Sanyasi R. G., Hill S.E., and Wolf B. “Shear Rheology and Filament Stretching Behaviour of Xanthan Gum and Carboxymethyl Cellulose Solution in Presence of Saliva.” *Food Hydrocolloids* 40 (2014): 71–75.

⁹Li Z., Yuan X.-F., Haward S.J., Odell J.A. and Yeates S., “Non-linear dynamics of semi-dilute polydisperse polymer solutions in microfluidics: effects of flow geometry”. *Rheologica Acta*, 50 (2011): 277-290.

¹⁰Riise C. and Belayneh M. “Characterization of the MWCNT-Duovis polymer composite effects on laboratory

water based drilling fluid”, *International Journal of NanoScience and Nanotechnology*, 10 (2019): 21-31.

¹¹Rocheffort W. E., and Middleman S. “Rheology of Xanthan Gum: Salt, Temperature, and Strain Effects in Oscillatory and Steady Shear Experiments.” *Journal of Rheology* 31, no. 4 (1987): 337–69.

¹²Gulrez S., Al-Assaf S., Fang Y., Phillips G., Gunning A., “Revisiting the conformation of xanthan and the effect of industrially relevant treatments.” *Carbohydrate Polymers* 90 (2012): 1235-1243.

¹³Souslov A., Curtis J.E., and Goldbart P.M. “Beads on a String: Structure of Bound Aggregates of Globular Particles and Long Polymer Chains.” *Soft Matter* 11, no. 41 (2015): 8092–99.

¹⁴Oliveira M.S.N, and McKinley G.H. “Iterated Stretching and Multiple Beads-on-a-String Phenomena in Dilute Solutions of Highly Extensible Flexible Polymers.” *Physics of Fluids* 17, no. 7 (2005): 071704.